Available online at www.sciencedirect.com
ScienceDirect
Journal of the European Ceramic Society 28 (2008) 1697–1713
www.elsevier.com/locate/jeurceramsoc

TiC–TiB_2 composites: A review of phase relationships, processing and properties

D. Vallauri [a,*], I.C. Atías Adrián [a], A. Chrysanthou [b]

[a] *Dipartimento di Scienza dei Materiali e Ingegneria Chimica, Politecnico di Torino, Corso Duca degli Abruzzi 24, 10129 Torino, Italy*
[b] *School of Aerospace, Automotive and Design Engineering, University of Hertfordshire, Hatfield, Herts AL10 9AB, United Kingdom*

Received 20 June 2007; received in revised form 15 November 2007; accepted 25 November 2007
Available online 11 February 2008

Abstract

Ceramic-matrix composites (CMCs) based on TiC–TiB_2 have attracted enormous interest during recent years because, in comparison to single-phase ceramics, they exhibit superior properties including high hardness, good wear resistance and high fracture toughness. This paper begins with a review of the TiC–TiB_2 equilibrium system and its possible influence on the processing and properties of the composite. The application of TiC–TiB_2 composites has been limited due to the fact that they have been difficult to process. Much of the research effort has therefore focused on the synthesis, processing and fabrication of TiC–TiB_2 and is based primarily on self-propagating high-temperature synthesis (SHS) and its derivatives, high-energy milling and sintering. The performance of SHS under the application of pressure has been the subject of particular investigation. These developments are the main subject of this review that also takes into account the resulting effects on the microstructure and the mechanical properties of TiC–TiB_2. The influence of the reaction parameters like reactant composition, reactant particle size and green density on the microstructure and properties is also reported.

Keywords: B. Composites; C. Hardness; C. Wear resistance; TiC–TiB_2; E. Cutting tools

1. Introduction

The development of ceramic-matrix composites (CMCs) is of increasing interest because they can enhance the intrinsically low fracture resistance of monolithic ceramics. Typical ceramic systems that are of such interest are carbide–boride composites of transition metals as they are recognised as valid candidates for technological applications under extreme conditions due to their excellent combination of mechanical and electrical properties as well as their good corrosion and oxidation resistance at high temperatures.[1] TiC–TiB_2 composites represent promising materials for use as wear-resistant parts like forming dies and cutting tools and also exhibit good behaviour as high-temperature structural components in heat exchangers and engines. In addition, the use of TiC–TiB_2 in non-structural applications like wall tiles in nuclear fusion reactors, cathodes in Hall–Heroult cells and vapourising elements in vacuum-metal deposition installations has been under investigation.[2,3] In comparison to conventional cermets based on WC and TiC, cermets based on TiC–TiB_2 composites, exhibit a higher hardness and chemical stability at high temperatures and are regarded as a good alternative for wear-resistant applications.[4]

Previous works had suggested that TiB_2 was superior for continuous cutting operations where high temperatures are developed in comparison to conventional tool materials.[5] However, this exceptional performance could not be substantiated[6] until the use of microstructural modification led to fine-grained TiB_2 cermets with improved and reliable cutting capability especially for steel machining operations.

It has also been shown that the fracture toughness and wear resistance of TiC–TiB_2 composites prepared from premixed TiB_2 and TiC powders were significantly higher than those of TiB_2 and TiC single phases.[7] Table 1 compares measurements of the Vickers hardness[6] between TiC–TiB_2 and single-phase TiC and TiB_2. It is evident that the TiC–TiB_2 hardness measured at room temperature was lower than that of the single-phase materials. However, at 600 °C the hardness of the composite exceeds the hardness of monolithic TiC and TiB_2. Such observations have

* Corresponding author. Tel.: +39 011 5644672; fax: +39 011 5644699.
E-mail address: dario.vallauri@polito.it (D. Vallauri).

0955-2219/$ – see front matter © 2008 Elsevier Ltd. All rights reserved.
doi:10.1016/j.jeurceramsoc.2007.11.011

Table 1
Vickers hardness at room and high temperature for TiC–TiB_2 composites and monolithic materials

Material	Vickers hardness (GPa)	
TiC	27.5 @ 25 °C	6.8 @ 600 °C
TiB_2	28.5 @ 25 °C	7.8 @ 600 °C
TiC–TiB_2	23.0 @ 25 °C	8.3 @ 600 °C

After Ref. 6

led to new research studies on the development of TiC–TiB_2 composites. The purpose of this publication is to review the recent developments in the processing of TiC–TiB_2 composites together with the effects on microstructural evolution and the subsequent properties.

1.1. Ti–C equilibrium phase diagram and crystal structure of titanium carbide (TiC)

The equilibrium Ti–C binary phase diagram as calculated by Frisk[8] from thermodynamic data obtained by Dumitrescu et al.[9] is shown in Fig. 1. Both the low temperature hexagonal modification of Ti (α) and the high-temperature body-centred cubic modification (β) allow a very limited amount of solubility of C in Ti. The equilibrium phase diagram exhibits only one carbide phase, TiC, that is characterised by a wide region of homogeneity (from $TiC_{0.48}$ to $TiC_{1.00}$) and melts congruently at 3068 °C.[10] Titanium carbide is characterised by a B1 (or NaCl-type) crystal structure where the titanium atoms are situated in a face-centred cubic closed-packed arrangement with the octahedral interstitial sites being occupied by the carbon atoms as shown in Fig. 2.[11] Non-stoichiometric TiC_{1-x} is disordered and occurs where some of the interstitial sites are vacant. A number of investigations have led to suggestions that through the redistribution of carbon atoms and structural vacancies, various ordered substoichiometric crystal structures may form in the Ti–C system.[12]

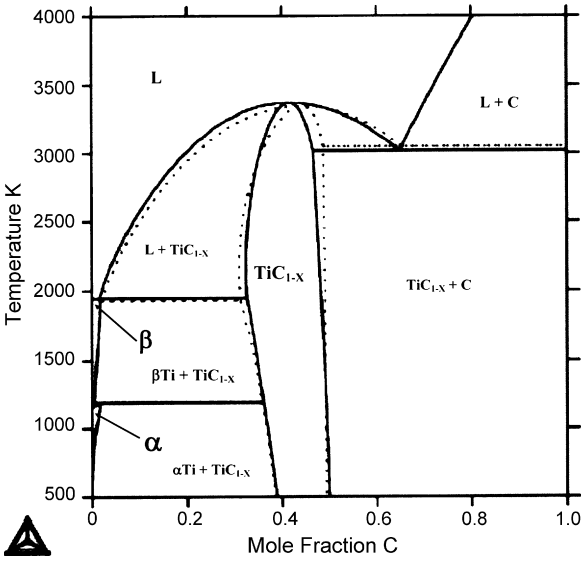

Fig. 1. The calculated Ti–C phase diagram by Frisk.[8] The dashed line shows the calculation using the description of Dumitrescu et al.[9]

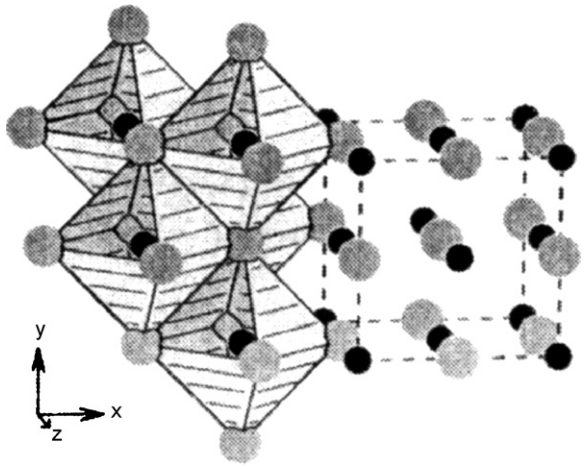

Fig. 2. Crystal structure of cubic TiC (NaCl type).[11] Copyright Wiley-VCH Verlag GmbH & Co. KGaA. Reproduced with permission.

Tashmetov et al.[13] observed two ordered structures with trigonal and cubic symmetry with compositions $TiC_{0.59}$ and $TiC_{0.62}$ respectively. The trigonal ordered phase was formed below 770 °C, while the cubic ordered phase was observed at higher temperatures. Lipatnikov et al.[12] have reported that $TiC_{0.6}$ can form a disordered phase. In addition, they reported the presence of Ti_2C with an ordered trigonal or cubic symmetry and another ordered Ti_3C_2 phase with orthorhombic symmetry. Two recent studies involving self-propagating high-temperature synthesis (SHS) or sintering of TiC-reinforced titanium-matrix composites, have claimed the existence of a distinct Ti_2C phase.[14,15] Wanjara et al.[14] who sintered Ti–6%Al–4%V and TiC powder mixtures between 1000 and 500 °C reported an interfacial reaction product of Ti_2C. Using lattice parameter measurements from neutron diffraction analysis, as well as quantitative analysis from low voltage field emission gun scanning electron microscopy, they concluded that the reaction product was stoichiometric Ti_2C with a B1 crystal structure. Ranganath and Subrahmanyam[15] who produced TiC-reinforced titanium-matrix composites also claimed the formation of Ti_2C with the same crystal structure. A similar phase was also observed by Chrysanthou et al.[16] during sintering of Ti–25 wt%TiC powders that were produced by SHS. Using lattice parameter measurements from XRD analysis, it was established that the SHS process had yielded disordered TiC_x, where x was about 0.65. During subsequent sintering, peaks equivalent to Ti_2C emerged. Inspection of the Ti–C equilibrium phase diagram indicates that the TiC phase in equilibrium with titanium would have the same composition as Ti_2C and therefore the XRD peaks from these studies would be expected to produce TiC_{1-x} of composition equivalent of Ti_2C. However, in the study by Chrysanthou et al.[16] what appeared to be very strange about this carbide composition was the emergence of new XRD peaks equivalent to Ti_2C, instead of peak broadening across the whole composition range of TiC_{1-x}. In spite of all these observations, the existence of a Ti_2C phase in the Ti–C system remains questionable, primarily because TiC_{1-x} can easily pick up oxygen to form titanium oxycarbides of various compositions. For example, in the work of

Table 2
Bulk properties at room temperature of titanium carbide (disordered state) with fcc structure and composition near 50 at% C[17]

Lattice parameter (nm)	0.43
Density (g/cm^3)	4.93
Melting point (°C)	3067
Micro-hardness (GPa)	28
Young Modulus (GPa)	450
Heat conductivity (W m^{-1} °C^{-1})	28.9
Linear thermal expansion coefficient (10^{-6} °C^{-1})	8.5
Electrical resistivity (μΩ cm)	100

Tashmetov et al.[13] levels of oxygen of up to 0.2 wt% have been reported. Whether this plays any role in stabilising these reported phases, remains unclear and requires further investigation.

1.2. Properties and applications of TiC

Transition metal carbides like TiC show a combination of properties including exceptionally high hardness, high melting point and relatively high electrical and thermal conductivities. As a result, these carbides have found a wide range of technological applications. In particular, TiC has refractory properties, is an abrasive material and also exhibits good resistance to high-temperature oxidation and to chemically corrosive environments. An overview of the most important properties of titanium carbide is presented in Table 2.[17]

Variations in the micro-hardness between bulk and thin film TiC are sometimes reported, probably due to the different dislocation density and grain size between the two forms.[17] Another factor that influences the micro-hardness is the chemical composition of the carbide. Specifically the micro-hardness of TiC_{1-x} increases with increasing carbon content. Single crystal investigations and orientation-dependent measurements on polycrystalline material of transition metal carbides have demonstrated the dependence of micro-hardness on crystal lattice orientation. For example, the Knoop hardness for TiC in the (1 1 0) plane is 27 GPa whereas that in the (1 0 0) plane is 31 GPa.[17]

The fcc carbides have been reported to show slip upon mechanical loading within the (1 1 1) plane in the {1 1 0} direction. The ductile-to-brittle transformation temperature for TiC has been measured to be around 800 °C and the carbide shows plastic deformation at relatively low temperatures of around 1000 °C. The yield stress for TiC has been demonstrated to follow the Hall–Petch relation.[17]

The most important industrial use of TiC is for wear-resistant applications by the cutting tool industry, in the form of a hard-metal or cermet. In fact TiC-based materials form the most important group of cutting tools after tungsten carbide–cobalt. Nickel is normally used as a binder metal for TiC, while small additions of Mo_2C are useful in extending the wettability between the carbide and the metallic phase. Applications in the form of spray coatings, deposited layers by PVD and CVD and diffusion layers for surface modified components[17] are also becoming important. In addition, TiC is also extensively employed in pumps for transporting molten materials, as a constituent in electrodes for oxy-electric cutting of steel and as thermocouples for use in reducing and inert atmospheres.[18]

1.3. Ti–B equilibrium phase diagram and crystal structure of titanium diboride (TiB_2)

The Ti–B equilibrium phase diagram has been the subject of several studies.[19,20] The phase diagram that is presented in Fig. 3 has been calculated by Murray et al.[20] The existence of three equilibrium boride phases (TiB, Ti_3B_4 and TiB_2) has been confirmed by Spear et al.[21] While Ti_3B_4 has been shown to be a line compound, both TiB and TiB_2 exhibit a small composition variation. There seems to be good agreement on the homogeneity range for TiB_2; according to Fenish,[22] this extends between 65.5 and 67 at% B, while Rudy and Windisch[23] measured 65.2 and 66.3 at% B and Thebault et al.[24] 65.5–67.6 at% B. These measurements were confirmed by observations of a small variation of the lattice parameters of TiB_2. There is agreement that TiB_2 melts congruently, however, there are discrepancies between various studies with regard to the melting temperature.

TiB_2 crystallizes with a hexagonal AlB_2-type structure with a *P6/mmm* space group. The boron atoms fill the trigonal prisms that are formed by the titanium atoms, as shown in Fig. 4.[11] Each boron atom has three boron neighbours in a trigonal planar arrangement, forming a two-dimensional honeycomb network with a distance of 0.175 nm.[11] The hexagonal symmetry of TiB_2 introduces anisotropy that makes the material difficult to sinter to full density without micro-cracking. As a consequence, TiC has been considered as a possible toughening second phase because it shows an appropriate thermodynamic compatibility, as well as, coherency with TiB_2[25] as shown in Fig. 5.

1.4. Properties and applications of TiB_2

TiB_2 is characterised by a high melting point, low specific weight, high hardness, high strength to density ratio, good wear resistance and excellent thermal and chemical stability up to 1700 °C.[26] Table 3 summarizes some of the properties

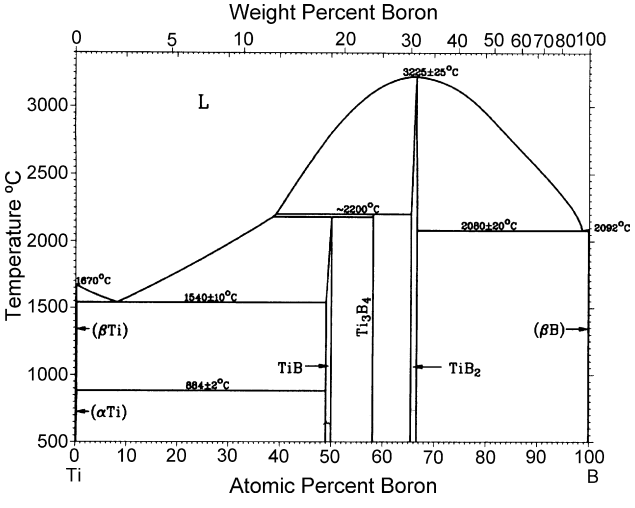

Fig. 3. Binary Ti–B phase diagram.[20] Reprinted with permission of ASM International®. All rights reserved. www.asminternational.org.

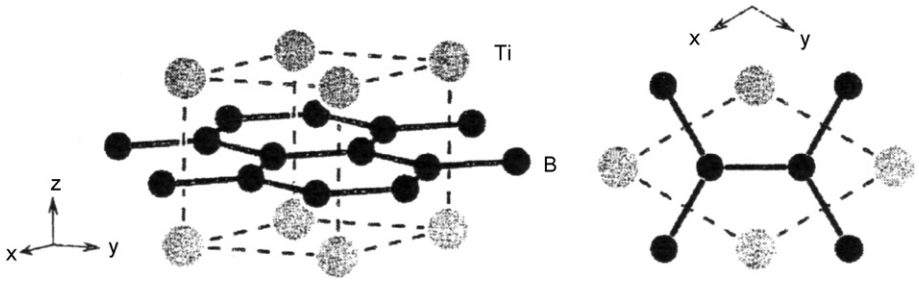

Fig. 4. The AlB_2 type structure of TiB_2 in a projection along the hexagonal axis (right) and a perspective view (left). The two-dimensional boron network (black) is highlighted.[11] Copyright Wiley-VCH Verlag GmbH & Co. KGaA. Reproduced with permission.

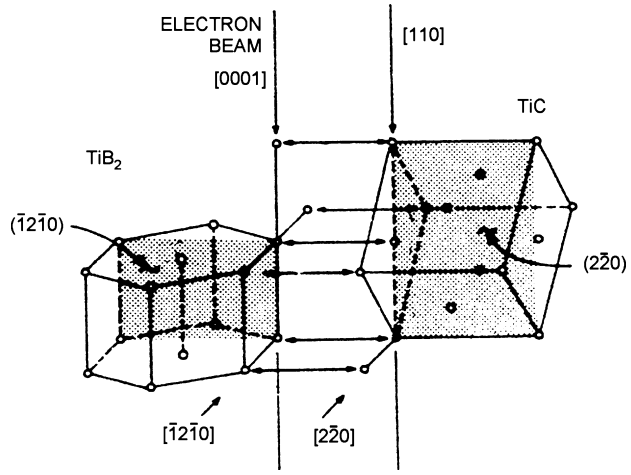

Fig. 5. Arrangement of titanium atoms at a precipitate–matrix boundary.[25] Copyright Wiley-VCH Verlag GmbH & Co. KGaA. Reproduced with permission.

of TiB_2. Single-phase TiB_2 ceramics have been used in the nuclear industry and for other specialised applications such as impact-resistant armour, crucibles and cutting tools. Multiphase TiB_2-based ceramics can also be used for such technological applications as wear components as well as cutting tools. Moreover, they are used as electrode materials, heating elements and sensors. Indeed, the electrical properties of TiB_2 have been extensively studied leading to the development of electrode materials, for example, for the extraction of aluminium.[6] Nevertheless, the wider application of TiB_2 is limited since the starting materials are expensive and the traditionally used sintering technique requires extremely high temperatures and long times.[17] Broader application of this material may further be inhibited due to concerns about the variability of the material properties.[27]

Table 3
Properties of TiB_2[6,27]

Lattice parameter (nm)	$a = 0.3028$; $c = 0.3228$
Density (g/cm^3)	4.52
Melting point (°C)	3225
Hardness $HK_{0,1}$ (kg/mm^2) (>95% dense)	2600 (25 °C) 2400 (200 °C) 1800 (400 °C) 1050 (600 °C) 460 (1000 °C)
Young modulus (GPa)	560
Friction coefficient	0.9
Wear coefficient	1.7×10^{-3}
Weibull modulus	11
Heat conductivity (W m^{-1} °C^{-1})	24–59
Linear thermal expansion coefficient (10^{-6} °C^{-1})	$5.107 + 1.997 \times 10^{-3} T$
Electrical resistivity (μΩ cm)	20.4 (25 °C) 26 (200 °C) 36 (400 °C) 46 (700 °C)

1.5. Equilibrium Ti–B–C ternary system

There have been a number of experimental studies[28,29] of the titanium–boron–carbon ternary system following the first thermodynamic estimate of the phase diagram by Brewer and Haraldsen.[30] A series of critical assessments followed,[23,28,29,31] the most important being the one conducted by Duschanek et al.[28] who calculated the phase equilibria above 1400 °C and up to the melting range. The Ti–B–C system involves only binary compounds as no ternary ones have been observed by any of the studies.

The combination of TiC and TiB_2 is thermodynamically stable up to 2600 °C where a pseudobinary eutectic reaction takes place. The various studies have reported coexistence between TiB_2 and TiC over a composition range. This is of course very important from the point of view of the properties, processing and performance of TiB_2–TiC composites and therefore a number of investigations have focused on the TiB_2–TiC pseudobinary section. However, there are some differences between the various studies with regard to the pseudo-eutectic temperature and composition. The properties of the composite TiC–TiB_2 critically depend on the binary Ti–C system, as the eutectic composition and temperature are dependent on the variation of the carbon content of TiC_{1-x}.[28]

Fig. 6 shows the pseudobinary phase diagram of the TiC–TiB_2 system as reported by Rudy et al.[31] The authors reported the eutectic temperature to be at around 2620 ± 15 °C and the composition at TiB_2–57 mol%TiC. The composition was subsequently corrected by the same authors to TiB_2–67.5 ± 2 mol%TiC.[23] According to Gusev,[29] the eutectic composition contains 59.8 mol% TiC and the eutectic temperature is at about 2663 °C. These values could be observed in the polythermal pseudobinary section $TiC_{1.0}$–TiB_2 (see Fig. 7). Duschanek et al.[28] have calculated the TiC–TiB_2 isopleth shown in Fig. 8, where good agreement with Gusev's[29]

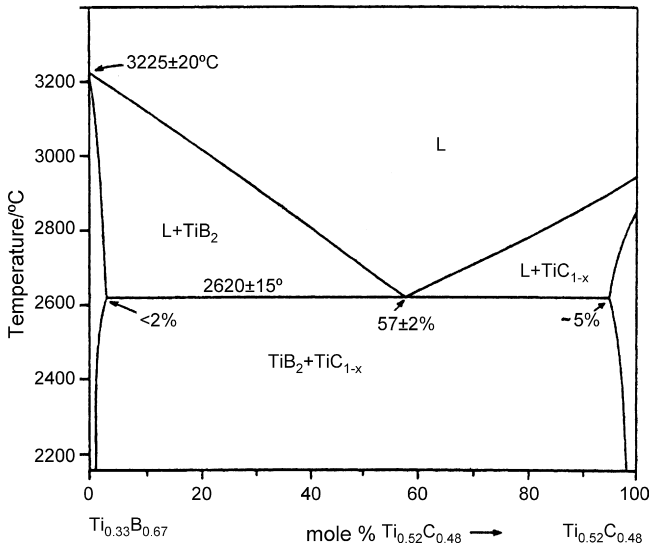

Fig. 6. Experimental phase diagram of the TiC–TiB_2 system.[31] Reprinted with permission of ASM International®. All rights reserved. www.asminternational.org.

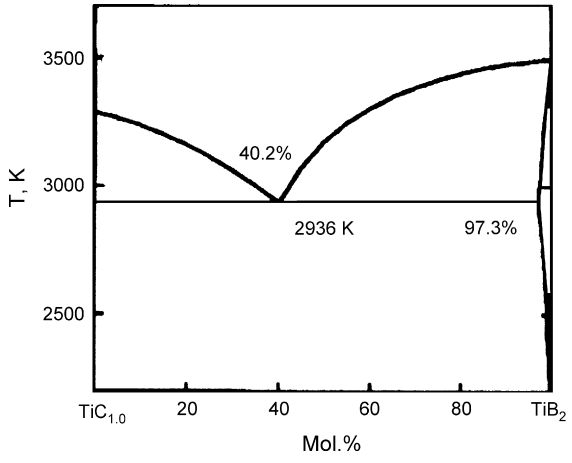

Fig. 7. Polythermal pseudobinary section $TiC_{1.0}$–TiB_2 calculated by Gusev[29].

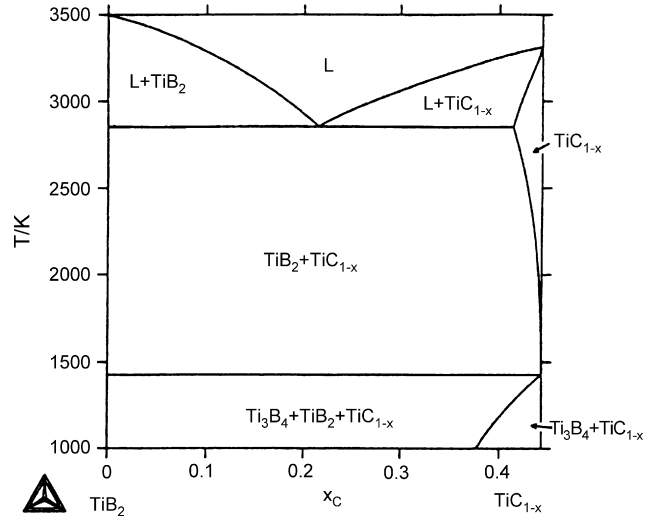

Fig. 8. TiC–TiB_2 phase diagram calculated by Duschanek et al.[28] ($x \cong 0.203$). Reprinted with permission of ASM International®. All rights reserved. www.asminternational.org.

work can be found for the reported eutectic temperature. In addition, the existence of Ti_3B_4 not considered in the work by previous researchers has been reported by Duschanek et al.[28] The highlighted differences are not significant considering that the methods of measurement at high temperatures are generally not very accurate. Concerning the solubility of the two constituents into each other, the values reported by Gusev[29] and Duschanek et al.[28] are lower than those previously presented.[29,31] Gusev[29] who calculated the pseudobinary section for $TiC_{1.0}$–TiB_2 reported that there is virtually no dissolution of TiB_2 in TiC, while Duschanek et al.[28] have reported that the maximum solubility of TiB_2 in TiC is 5 mol%, at an eutectic temperature of 2620 °C. On the other hand, Gusev[29] showed that the solubility of TiB_2 in $TiC_{0.8}$ is 5.3 mol% indicating the importance of the carbide composition on the dissolution behaviour. According to Gusev[29] the solubility of $TiC_{1.0}$ and $TiC_{0.8}$ in TiB_2 extends to 2.7 and 3.2 mol% respectively.

1.6. Coherency of TiC–TiB_2 composites

Holleck et al.[26] have suggested that TiC–TiB_2 composites could establish coherency between their most densely packed lattice planes (see Fig. 5). In fact, Sorrell et al.[32] using values of the lattice parameters reported by Rudy and Windisch,[23] estimated the lattice mismatch between TiB_2 and TiC to be only about 1.6%. This value was much lower than the critical value of 16% that is required for a semi-coherent interface. The favourable interfacial match in the composite material has been reported to allow good densification of TiC/TiB_2 composites during sintering.[33] One of the reported advantages of the common coherency between the $(1\,1\,1)_{TiC}(0\,0\,0\,1)_{TiB_2}$ particle interfaces[6] was the contribution to phase boundary toughening that led to the superior wear resistance of TiC–TiB_2 in comparison to the monolithic ceramics during milling of steel.

2. TiC–TiB_2 synthesis and processing

2.1. Processing routes

Ceramic-matrix composites are usually prepared by the densification of mechanically mixed component powders. Since the melting temperatures of TiB_2 and TiC are extremely high, their fabrication to full density requires long exposures at high sintering or hot-pressing temperatures. The densification of such materials is made even more difficult due to their high degree of covalent bonding and the low self-diffusion coefficients of the constituent elements. The high processing temperatures adversely affect the microstructure due to grain growth and also lead to high production costs. As a consequence, there is an increasing need for a more practical route of fabricating TiC–TiB_2 CMC parts.[34]

The fabrication of TiB_2/TiC nanocomposite powder via high-energy ball milling processing was reported by Li et al.[35] The authors observed that ball milling a mixture of B_4C and elemental Ti powders in Ar gas atmosphere at ambient temperature using hardened steel 5 mm balls resulted in the formation of

TiC prior to the formation of TiB_2, due to the faster diffusion of carbon relative to boron in titanium.[36] The complete formation of TiC and TiB_2 was accomplished after 5 h of milling. The final product consisted of nanosized TiC particles and microscale TiB_2 particles.

According to Mogilevsky et al.[37] between 0 and 4.5 h of milling, a small amount of B_4C decomposed into boron and carbon and the initial reaction:

$$Ti + B_4C \rightarrow Ti + 4B + C \rightarrow TiC + 4B \quad (1)$$

took place. In fact all the B_4C peaks had disappeared after 2 h of milling. This observation led Li et al.[35] to the conclusion that B_4C had decomposed to boron and carbon prior to the emergence of TiC (after 4 h of milling). However, as pointed out by the authors[35] the main B_4C peak may have been shielded by the one of the titanium peaks. The XRD data presented no evidence of elemental boron and carbon. Both of these have a lower atomic mass than titanium and, if present, their XRD peaks are expected to be much less intense than those of the metal and might have been shielded by those of titanium. Li et al.[35] did not consider the possibility of loss of carbon from B_4C to form other lower carbon-containing boron carbides like $B_{13}C_2$, etc. as part of the reaction mechanism. While Eq. (1) is thermodynamically feasible, in any analysis, it is also necessary to consider the formation of TiB_2. This can be done by using chemical thermodynamic data compiled by Kubaschewski and Alcock[38] in order to examine the stability of TiC in relation to TiB_2 as presented below:

$$2TiC + B_4C \rightarrow 2TiB_2 + 3C,$$
$$\Delta G^\circ = -191,300 + 17.5T\,(\mathrm{J/mol}) \quad (2)$$

$$TiC + 6B \rightarrow TiB_2 + B_4C,$$
$$\Delta G^\circ = -384,400 + 30.9T\,(\mathrm{J/mol}) \quad (3)$$

$$TiC + 2B \rightarrow TiB_2 + C,$$
$$\Delta G^\circ = -131,400 + 3.8T\,(\mathrm{J/mol}) \quad (4)$$

The Gibbs' Free Energy data for the above reactions involving reactants and products in their standard state, suggest that TiC, at the temperatures encountered in the study, will not be stable in the presence of boron or B_4C as TiB_2 will form instead. However, from the microstructural evidence provided by Li et al.[35] there is no doubt that the formation of TiC from B_4C (or from carbon in the presence of boron) without any formation of TiB_2 does indeed take place during the early part of the reaction. The reason for this observation is likely to be due to kinetic factors.

The synthesis of TiB_2/TiN/Ti(C_xN_{1-x}) nanocomposite powders by means of high-energy ball milling followed by heat treatment was also reported by the same authors.[39] After 30 h of milling, the reaction $Ti + B_4C + BN + B$ (amorphous) took place, and the resulting powder mixtures were mainly composed of nanocrystalline TiN, TiC and TiB_2 with some unreacted Ti remaining. Following subsequent heat treatment at 1300 °C, the as-milled powder was transformed to the final product that was composed of nanosized TiB_2 and TiN/Ti(C_xN_{1-x}) particles.

Reaction sintering and hot pressing with or without sintering aids are fabrication techniques employed for the production of dense solid bodies of TiC/TiB_2 ceramics.[40] Since the melting points of both TiC and TiB_2 are in excess of 3000 °C, both methods require either high sintering temperatures or liquid-forming additives. Expensive techniques, requiring the application of pressure are normally required to achieve densification at reasonable temperatures without the use of a binder. At high temperatures, grain growth becomes predominant, whereas during the liquid phase sintering, a low melting phase is produced at the grain boundaries. The addition of carbides was reported to be useful in the inhibition of grain growth during the hot-pressing of Ti($C_{0.5}$, $N_{0.5}$)–30 wt%TiB_2.[41] Small contents (5 wt%) of ZrC, HfC or NbC to the binary system reduced the optimum sintering temperature by 100 °C down to 1600 °C and also significantly narrowed the transverse rupture strength distribution of the sintered specimens (the Weibull coefficient improved from 8 to 12). The above phenomena are conceivably due to the fact that the added HfC particles react with the Ti(C, N) particles to form Hf-rich (Hf, Ti) (C, N) or Ti-rich (Ti, Hf) (C, N) solid solutions which limited the grain growth. The lower sintering temperature of the system was also reported to suppress the grain growth.

Pressureless sintering with the addition of metal binder phases is used for the fabrication of TiC/TiB_2 based cermets. The metal binders used are generally based on Ni and Fe, that exhibit good capability of dissolving TiC and TiB_2 respectively. Ogwu and Davies[25] have attempted to achieve densification and some ductility in a TiC/TiB_2 cermet prepared by pressureless sintering for 90 min at 1550 °C, by using a (Ni + X) based binder where "X" represents a binder additive. The same authors had previously reported that molybdenum is a potential binder additive.[42] The authors give two possible reasons for this; molybdenum either hybridises its outermost d- and s-electrons in its reaction to reduce the contact angle in the system or simply donates its single s-electron. The binder selected gave a good densification in the composite, as a good wettability of the TiC and TiB_2 grains by the binder alloy was observed. The hardmetals obtained with (Ni + X) exhibited densities higher than 90% theoretical density, whereas a maximum value of 75% theoretical density was attained for sintering at 1550 °C for 90 min with no binding additives.

Singh et al.[43] reported the fabrication of porous TiC/TiB_2 cermets by liquid phase sintering in an atmosphere of hydrogen at 1300–1350 °C for 1 h through the addition of a binder system based on Ni/Mn alloys. The binder modification was designed in order to lower the melting point of pure nickel by alloying with manganese. Mo_2C was also employed as sintering activator, as the TiC–Mo_2C system exhibits better wettability with Ni as compared to TiC. The replacement of the nickel binder with nickel–manganese enhances densification due to its better wetting and solubility ratio compared to nickel. The lower melting point of the Ni–Mn alloy (1020 °C) compared to nickel

(1453 °C) resulted in a significant reduction in viscosity thus promoting better densification.

As previously reported, the processing of these ultra refractory composites into components with full density through traditional routes requires extremely high temperatures. A number of new densification techniques have thus been investigated to overcome this problem. For example, transient viscous sintering in mullite-matrix composites,[44] reactive hot pressing (RHP) by using displacement reactions,[45] addition of "tailored" sintering aids in TiB_2–TiC composites,[33] self-propagating high-temperature synthesis assisted by a forced consolidation step[46] and directional reaction of molten titanium with a B_4C preform.[47]

TiC/TiB_2 with and without Ni addition were fabricated by a reactive hot pressing process also referred to as displacement reaction under pressure.[4,34,48] The process was carried out using Ti + B_4C(+Ni) powder blends at a temperature of 1100 °C which is considerably lower than the temperatures that are typical of conventional consolidation methods for ceramic-matrix composites. The RHP products with Ni addition were fully dense, whereas a final density of 95% theoretical density was achieved in the Ni-free material.

Zhao and Cheng[1] have studied the formation of TiC–TiB_2 composites by reactive sintering from a starting powder mixture of Ti and B_4C. In this technique both the chemical reactions between the starting materials and the densification occur simultaneously in a single firing step.[49] The authors reported that the firing time had a significant effect on the chemical reactions of the system, indicating the importance of diffusion phenomena in the reactions. Complete reaction was achieved at 1500 °C after 1 h.

TiC/TiB_2 bulk composites were alternatively fabricated by floating zone (FZ) directional solidification of TiC and TiB_2 powder blends of eutectic composition in two separate studies.[32,50] Unlike many other ceramic fabrication processes, the directional solidification of eutectic compositions affords the advantage that the resultant microstructures are not dependent on the particle size or shape of the starting materials, but rather are related to the solidification conditions. These aligned composites exhibited enhanced bonding between the phases and a high level of thermal stability as a result of *in situ* growth processing. These features led to superior physical properties for many high-temperature applications.

Other researchers[3,36] have used the Transient Plastic Phase Processing (TPPP) technique in which Ti metal is exploited as a transient plastic phase. The TiC/TiB_2 composite was produced in two stages; during the first stage pressure was applied to shape and fully densify the reactants at medium temperatures (around 800 °C) while the transient phase was soft, i.e. before reaction. Once the reactants were densified the reaction was allowed to proceed, forming a new phase *in situ* and rendering the matrix more refractory. Following this procedure, TiC–TiB_2 and $TiC_{0.6}$–TiB_2–Ti_3B_4 composites were hot-pressed to full density and complex net- or near-net shapes at temperatures as low as 1600 °C and moderate pressure (40 MPa) using starting mixtures of Ti/B_4C and $TiC_{0.5}$/TiB_2 respectively. The transient plastic phase in the former case was Ti while in the latter it was $TiC_{0.5}$. The compressive yield strength of TiC_x at 1200 °C is in fact reported to drop from ~430 to ~60 MPa as x decreased from 0.93 to 0.66.[51]

2.2. Self-propagating high-temperature synthesis

Self-propagating high-temperature synthesis is based on highly exothermic reactions, which upon initiation becomes self-propagating. Many ceramic materials including TiC and TiB_2 can be synthesized by means of SHS.[47] The products of the process are porous and therefore have to be compacted and sintered to produce bulk components suitable for engineering applications.[16] The SHS process is characterised by several advantages including fast reaction rates, low power consumption and high-energy efficiency provided by the exothermic reactions.[52] An additional attraction is the ability to apply pressure on the products during synthesis and this can simultaneously lead to densification of monolithic and composite materials.[52] The highly exothermic reactions (for example, the reaction between Ti and C produces an exothermic energy equal to 183.1 kJ/mol) become self-sustaining after they have been initiated by a low energy input (ignition). The high combustion temperature allows the volatilisation of the impurities, which are expelled as the reaction wave propagates through the sample. As a consequence, high purity products are obtained.[53,54] Fig. 9 shows experimental results on the relationship between the particle size of titanium and the wave velocity in the synthesis of TiC and TiB_2.

The direct reaction between Ti and B_4C to produce TiC–TiB_2 composites is highly exothermic ($\Delta H^\circ = -686$ kJ/mol), and is capable of generating temperatures exceeding the pseudo-eutectic temperature in the TiC–TiB_2 system of 2620 °C. The wave-front propagation velocity has been observed by Agrafio-

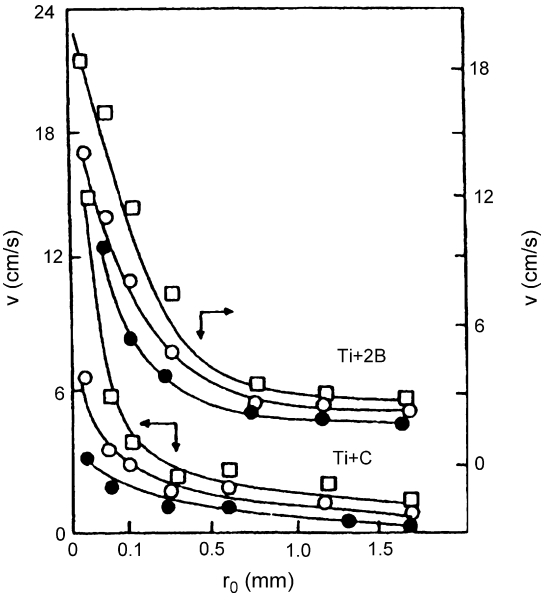

Fig. 9. Dependence of the combustion rate of Ti + 2B and Ti + C mixtures for self-propagating high-temperature synthesis (SHS) on the Ti particle size for several initial temperatures (20, 200 and 400 °C).[52] Copyright Wiley-VCH Verlag GmbH & Co. KGaA. Reproduced with permission.

tis et al.[55] to depend upon the particle size of reactants. Only two phases were detected (TiB_2 and TiC) in the combustion products when B_4C powders with particle size <8 μm and Ti with size <55 μm were used. A brittle product exhibiting a partial melting on a particle level was obtained when very fine B_4C powder was used. For coarser B_4C and Ti powders, other phases such as Ti_3B_4 and TiB were also formed.

The SHS process allows the *in situ* synthesis of multi-phase materials, as in the case of TiC–TiB_2 composites. This important feature remarkably affects the product characteristics, since materials produced by SHS exhibit outstanding properties that are often better that those exhibited by the same composites produced by conventional routes (i.e. pre-mixing of TiC and TiB_2 powders). In the case of the simultaneous synthesis of TiC and TiB_2 by SHS, the reaction mechanism is characterised firstly by the formation of the TiC phase.[56] The chemical thermodynamic analysis presented earlier in this review suggests that this is due to kinetic factors. The heat released by this reaction is sufficient to ignite the reaction for the formation of the TiB_2 phase and to sustain the self-propagating front, as observed by time-resolved XRD examination following ignition of the reaction from elemental powders.[56] The overall process is speeded up by the melting of Ti.

The possibility of synthesizing TiC_{1-x}/TiB_2 nanostructured powders by a metastability route based on the SHS process followed by quenching was also investigated.[57] The reactant stoichiometry was optimised in order to have an SHS reaction characterised by a combustion temperature that was higher than the eutectic temperature of the system. The rapid cooling, by means of quenching in liquid nitrogen, of the SHS products immediately following the reaction yielded inherently nanostructured powder agglomerates. The metastable nature of the products allowed the conversion of the nanostructured powders into a stable, fine-grained (nanocomposite) microstructure upon recrystallization following heat treatments at moderate temperatures.[58] The SHS-quench process led to the formation of powder agglomerates characterised by fine structures, as shown in Fig. 10.[59] A certain degree of metastability of the SHS-quench

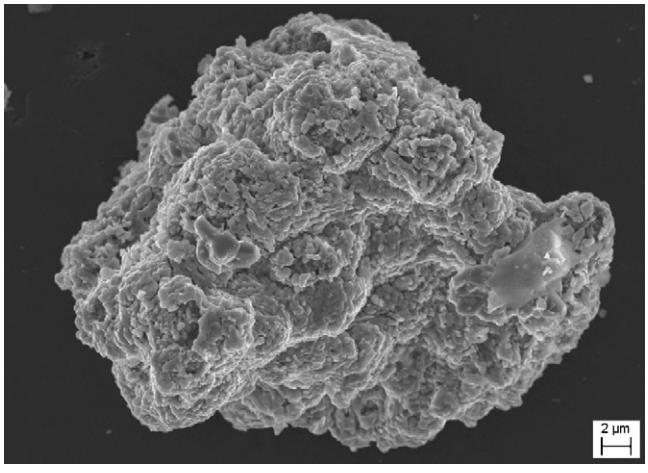

Fig. 10. SEM photographs of TiC_{1-x}–TiB_2 powder products obtained by SHS-quench process.[59]

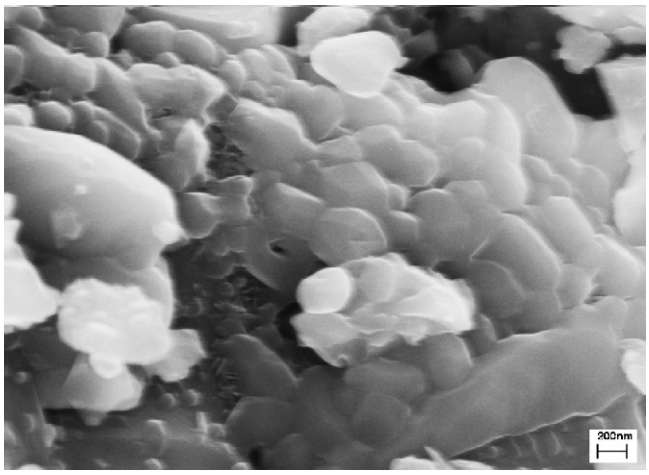

Fig. 11. SEM photographs of TiC_{1-x}–TiB_2 powder products obtained by SHS-quench process showing the re-crystallization after annealing for 1 h at 1200 °C.[59]

products was observed after thermal treatments, as confirmed by the morphological evolution of the nanostructures induced by annealing of the powders at 1200 °C for 1 h. The retainment of fine grains was possible thanks to the metastability of the starting materials (Fig. 11).

If the SHS process is conducted under the application of pressure, it is possible to achieve synthesis and densification simultaneously.[34] This process is commonly referred to as high-pressure self-combustion synthesis (HPCS) and has been used in a number of studies[60–62] to consolidate TiC–TiB_2 composites. HPCS of Ti/B_4C/C starting mixtures led to maximum densities of 96[60] and 96.8%.[62] The achievement of higher theoretical density between 98 and 99% was reported by Bhaumik et al.[40] using the same process starting from elemental powders and a 3 GPa pressure in the temperature and time ranges of 1977–2477 °C and 5–300 s. A minimum ignition temperature of 1977 °C was required to make the reaction self-sustaining. Even though the reaction ran to completion after ignition with no further supply of energy from the external source, the authors reported the necessity to maintain a high temperature for better densification.

Using similar methods, dense TiB_2–TiC composites have been fabricated by direct reaction of molten titanium with boron carbide preforms in the presence of a small weight percentage of nickel.[4,34,48] The studies reported the synthesis of TiC–TiB_2–Ni composites by pressure-assisted thermal explosion, which is a particular mode of conducting combustion synthesis reactions. The reactive synthesis was carried out starting from fully dense Ti–B_4C preforms with or without Ni binder additive obtained by high-pressure consolidation/cold sintering (3 GPa, 300 °C). The ignition temperature, T_{ig}, was reported to be about 950 °C. Ignition was believed to be achieved as a result of melting of titanium due to the presence of a low melting eutectic (∼940 °C) in the Ni–Ti system. The thermal explosion experiments were carried out in a rigid die preheated to 1000 or 1100 °C and subjected to a pressure of 150 MPa. Thermal explosion occurred after about 15–20 s after pressure had been applied. After explosion of the reaction, the sample continued to be held under pressure for

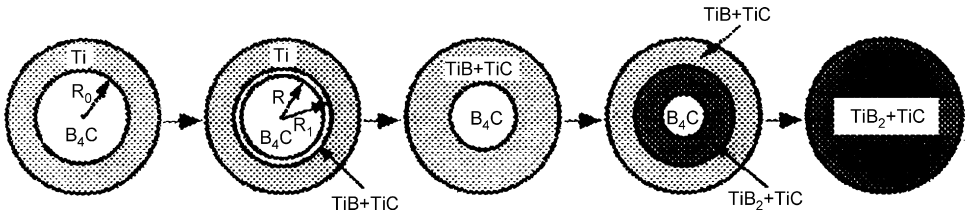

Fig. 12. Schematic drawing of the model geometry and sequence of reaction products around a spherical B_4C particle in B_4C–3Ti powder blend.[65]

1 min and then unloaded and removed form the die. The overall process duration was observed to be about 2 min.

Dense TiB_2 and TiC compacts have also been fabricated by self-propagating synthesis in combination with dynamic compaction (DC)[63] of elemental powders. This process utilizes an exothermic, condensed phase combustion synthesis to form a hot and porous ceramic body. The reacted, still hot body is then consolidated to high density by the action of a pressure wave from the detonation of a high explosive hence the term dynamic compaction. TiC and TiB_2 samples have been produced by SHS/DC achieving a theoretical density of 98.0% and micro-hardness values[64] which were equal to or greater than commercially available monolithic hot-pressed materials.

2.3. Microstructural aspects

The microstructure of TiC–TiB_2 bulk materials reported in the literature is greatly affected by the processing routes employed. In spite of the extremely high temperatures required for densification, the microstructures obtained can be fine grained, but are rarely characterised by crystal grains finer than 1 μm. Singh et al.[43] reported that TiC–TiB_2 cermets in a Ni–Mn binder and small additions of Mo_2C showed significantly increased wetting behaviour when compared to the same material without the presence of Mn. The emergence of the refractory TiC–Mo_2C carbides was reported to be efficient in inhibiting the grain growth of TiB_2, as confirmed by the experimental data showing a lower grain size of the boride phase in the composite containing TiC–Mo_2C (6.9 μm for TiB_2–TiC–Mo_2C–40 wt%Ni/Mn) with respect to the composite containing only TiB_2 (9.9 μm for TiB_2–40 wt%Ni/Mn).

Gotman et al.[34] obtained a TiC–TiB_2 composite by simultaneously performing SHS and densification using a B_4C–3Ti powder blend. However, the resulting microstructure was not fully homogeneous. Finer areas characterised by a grain size slightly larger than 1 μm were observed at the periphery of the sample, whereas a coarser microstructure was observed in the centre suggesting a lower maximum temperature on the surface due to the contact with the pressure die. Near full density samples were obtained. The material was pore-free with the brighter TiC and darker TiB_2 phases being easily distinguishable. The microstructure consisted of equiaxed TiC grains and TiB_2 platelets with an aspect ratio of 2. The authors also developed a model that suggested that the formation of the microstructure during pressure-assisted SHS, occurred by the reaction taking place at the contact points between the Ti and B_4C particles. A schematic diagram describing this is shown in Fig. 12.[65] The model analysis showed that the B_4C particle size had a significant effect on the ignition of the thermal explosion, as was also observed by Agrafiotis et al.[55]

The composites obtained by HPCS[40] exhibited a uniform microstructure consisting of equiaxed grains of TiB_2 and TiC of relatively fine grain size.

Besides the grain size and microstructural homogeneity, the shape of the resulting phases of the composite material also differed depending on the fabrication process. This difference was highlighted in Fig. 13, where rounded ceramic grains can be observed in a TiC–TiB_2 composite obtained by reactive sintering at 1750 °C.[1] In fact, the TiB_2 platelets usually observed in the materials obtained by technologies characterised by lower processing times were not distinguished in this case. This indicated the importance of diffusion in this kind of process. Therefore, the microstructure of TiC–TiB_2 composites was significantly affected by the fact that the diffusivity of carbon was significantly greater than that of boron.[66] The product particles were relatively large (~5 μm) when fired at 1500 °C for 5 min, but interestingly, the particle size of the final products at 1750 °C was actually refined and in fact even smaller than those of the starting reactants. A schematic diagram of the mechanism of the reactive sintering process was proposed as reported in Fig. 14. The reaction mechanism involved the formation of intermediate TiB and Ti_3B_4 phases that were subsequently fully converted into the TiC and TiB_2 products. Increasing temperature and time accelerated diffusion and promoted TiB to convert into TiB_2,

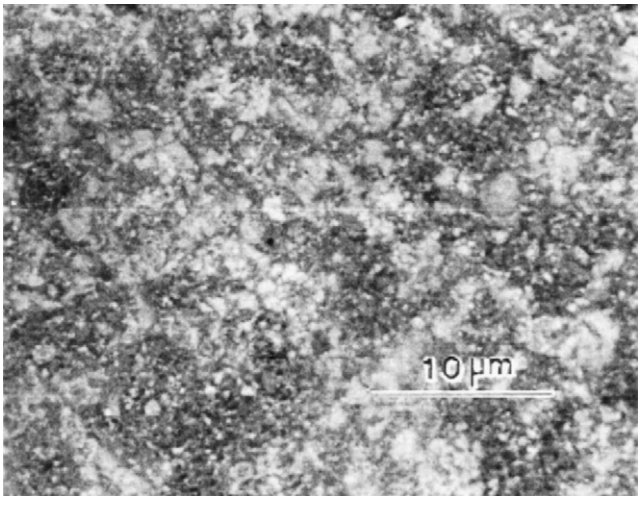

Fig. 13. Microstructure of TiB_2/TiC composite obtained by reactive sintering, 5 min dwell time at 1750 °C.[1]

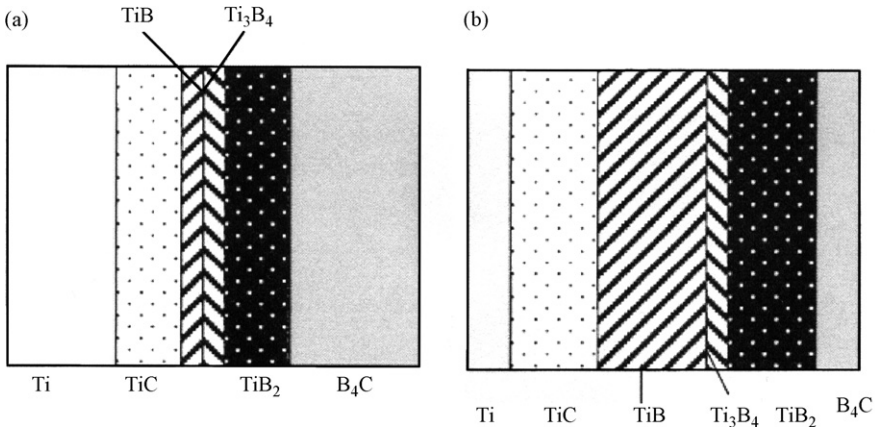

Fig. 14. Schematic diagrams of reaction $3Ti + B_4C = 2TiB_2 + TiC$ at (a) low temperatures and (b) high temperatures.[1]

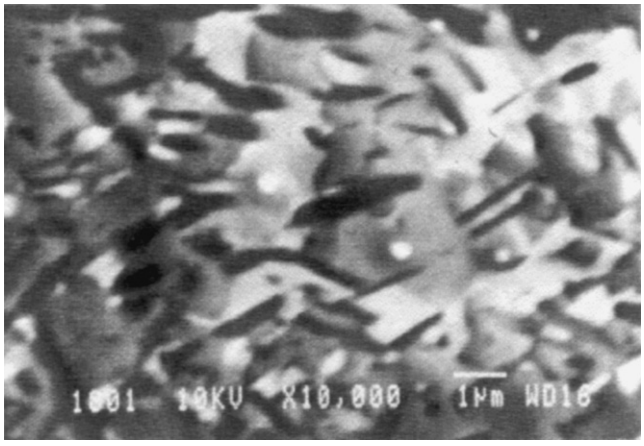

Fig. 15. A representative microstructure of the composite material synthesized via RHP from dense B_4C–3Ti powder blend.[34]

leading to the much more homogeneous microstructure that is shown in Fig. 13.

The use of reactive hot pressing for 4 h at 1100 °C[34] yielded composite materials with finer microstructures as shown in Fig. 15, however full conversion of the starting materials into TiC–TiB_2 composites was not achieved. In fact, undesired phases, like TiO_2 and possibly TiN, were detected in the product materials.

Bulk TiC/TiB_2 composites with different compositions were obtained by means of floating zone directional solidification,[50] observing the formation of an interesting eutectic structure. Spherical TiC grains of 2 μm in diameter co-existing with eutectic texture were observed at a composition of 20 mol%TiB_2–80 mol%TiC (Fig. 16a) indicating that the TiC content was higher than that of the eutectic composition. The microstructure of 60 mol%TiB_2–40 mol%TiC composite consisted of prismatic TiB_2 grains of 1.2 μm in width and eutectic phase (Fig. 16b). The authors reported a eutectic composition of 28 mol%TiB_2–72 mol%TiC and the composites with this composition prepared by the FZ method exhibited the microstructure shown in Fig. 17.

The TiB_2–TiC eutectic composite showed a lamellar texture where TiB_2 platelets were dispersed in the TiC matrix. The TiB_2 platelets had a thickness of 600 nm and length of 1–4 μm and were uniformly dispersed in the TiC matrix. The microstructure of the eutectic composite showed significant orientation along the growth direction (Fig. 17b). An increase in the grain size of the TiB_2 and TiC phases was observed by reducing the solidification rate leading to an increase of the growth rate.

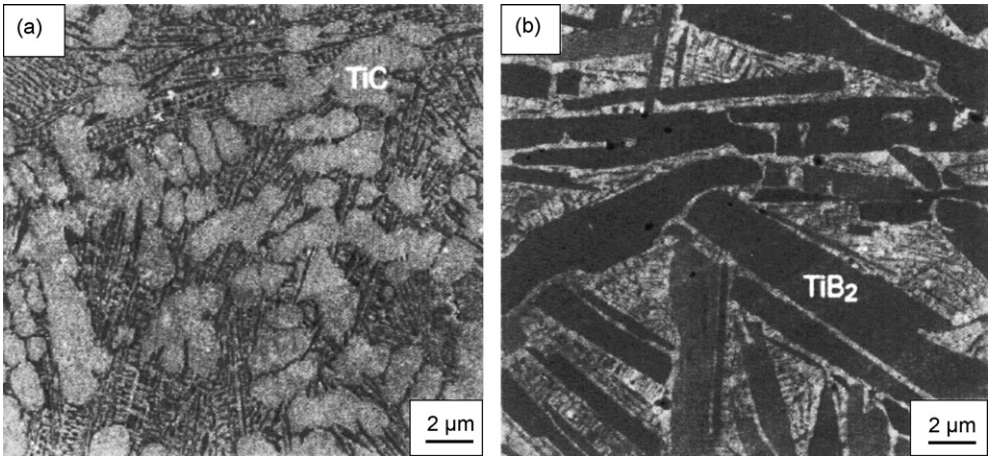

Fig. 16. Microstructure of TiB_2–TiC composites prepared by floating zone directional solidification at the composition of 20TiB_2–80TiC (mol%) (a) and 60TiB_2–40TiC (mol%) (b).[50]

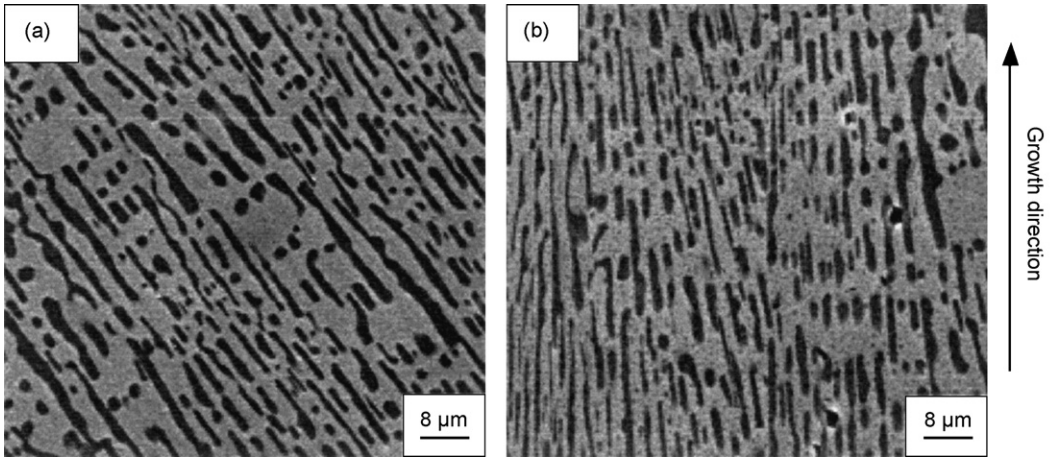

Fig. 17. Microstructure of TiB_2–TiC composites with eutectic composition ($28TiB_2$–72 mol%TiC) prepared by floating zone directional solidification for cross-section perpendicular (a) and parallel to the growth direction (b).[50]

The microstructural evolution during Transient Plastic Phase Processing of TiC–TiB_2 composites reported in a number of papers[2,36] is characterised by the presence of three equilibrium phases, namely TiC_{1-x}, TiB_2 and Ti_3B_4. The authors developed a model describing this microstructural evolution at various processing steps, i.e. at various temperatures, as presented in Fig. 18.[3] In particular, the formation of equiaxied TiB_2 grains and of a Ti_3B_4 platelet-like phase was reported.

The fabrication of bulk TiC–TiB_2 composites characterised by nanostructure has been obtained by Lee et al.[67] through field-

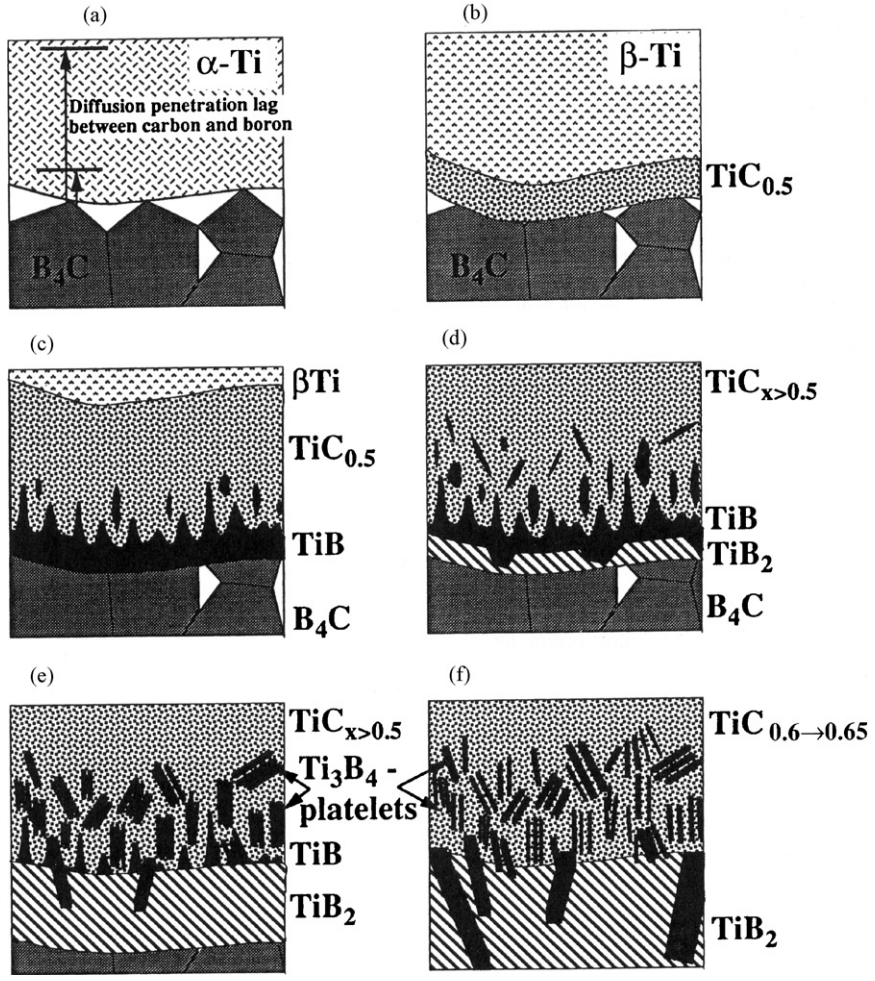

Fig. 18. Microstructural evolution model for TiB_2/TiC composites fabricated by TPPP.[3] (a) 800 °C; (b) 920–1000 °C; (c) 1000–1300 °C; (d) 1300–1450 °C; (e) 1450–1600 °C; (f) 1600 °C soak.

activated synthesis under pressure from high-energy ball milled Ti + B + C reactants. It was observed that the process greatly influenced the grain size of the final composite. Near full-density composites with crystallite size of the order of about 50 nm were achieved.

3. Properties and applications of TiC–TiB_2 composites

TiB_2 and TiC are important materials for high-temperature applications because of their high melting point, hardness, elastic modulus and electrical conductivity and relatively low coefficient of thermal expansion. The favourable interfacial match between TiB_2 and TiC is assumed to encourage a high mobility of atoms across the interface, leading to a significant enhancement in properties and in particular improvement in fracture toughness.

3.1. Mechanical properties of TiC–TiB_2 composites

Bulk TiC–TiB_2 composites have been reported to present an excellent wear resistance when produced by hot pressing or even by pressureless sintering of eutectic compositions at 1600–1700 °C.[6,28] TiC–TiB_2 composites prepared by Holleck et al.[68] also have shown excellent wear resistance and improved fracture toughness. The fracture toughness of the material is also expected to improve due to good interfacial coherence that exists between TiC and TiB_2.

For TiC–TiB_2-based cermets, fracture analysis of composites with (Ni + X) binder obtained by pressureless sintering,[25] revealed a crack propagation preferentially located in the TiB_2 grains and at TiC/TiB_2 interfaces with occasional transgranular fracture and good cohesion between the hard particles and the matrix. This was attributed to the improved wetting and bonding that were expected to result through the addition of the Ni + X binder. A predominantly ductile tearing mode was observed on the fracture surface of the TiC–TiB_2 composite sintered with 5 wt% (Ni + X) binding additive. The optimised sintered TiC–TiB_2 composite showed promising behaviour in terms of wear resistance, as demonstrated by the low wear loss of the material observed during pin-on-disc tests.[69]

In the case of TiB_2–TiC–Mo_2C–Ni–Mn cermets,[43] the significant improvement in the bending strength that was reported by Singh et al.[43] was attributed to multiple slip systems possessed by TiC[33] and its better densification as compared to TiB_2-based cermets.

A high value of micro-hardness of ~25 GPa was measured by Gotman et al.[34] in fully dense TiB_2–TiC–Ni composites manufactured from B_4C + Ti + Ni blends. The composite also exhibited a high value of fracture toughness of 11 MPa $m^{1/2}$, indicating the toughening effect of the finely dispersed Ni phase. The hardness of the TiB_2–72 mol%TiC composite obtained by floating zone directional solidification[50] was 23–26 GPa. The hardness of the composites increased with increasing TiC content, as shown in Fig. 19. The crack propagation in the composite was in a mixed transgranular and intergranular mode. The TiB_2–TiC composites with higher contents of TiB_2 were reported to have a slightly higher fracture toughness because of the intergranular fracture.

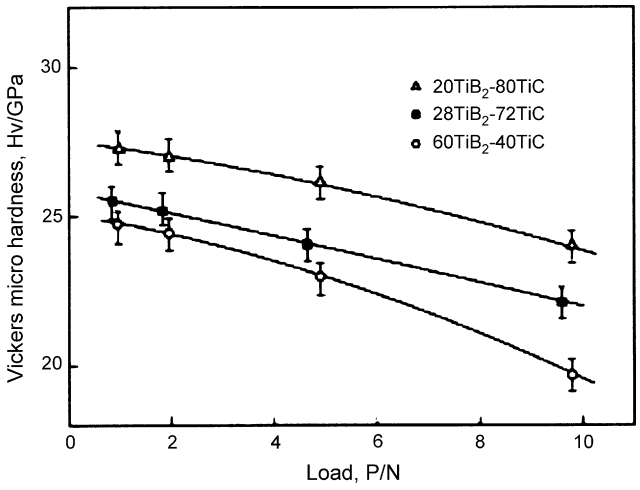

Fig. 19. Load dependence of Vickers micro-hardness of TiB_2–TiC composites obtained by floating zone directional solidification at the composition of 60TiB_2–40TiC (mol%) (a), 28TiB_2–72TiC (mol%) (b) and 20TiB_2–80TiC (mol%) (c).[50]

As for TiC–TiB_2–Ti_3B_4 composites fabricated by Transient Plastic Phase Processing,[3,36] the fracture toughness and strength were observed to be enhanced by the formation of Ti_3B_4 platelets with respect to those of the equiaxed composite. The superior fracture toughness was attributed by Brodkin et al.[70] to the interaction of Ti_3B_4 platelets with the propagating crack through well-known mechanisms of fracture energy dissipation by crack deflection, grain bridging, debonding and pullout. The occurrence of a mixed intergranular–transgranular fracture mode was observed by examination of the fracture surfaces. The authors[70] also evaluated the influence of temperature on the mechanical properties of TiC–TiB_2 composites fabricated by TPPP. The temperature dependencies of the K_{Ic} values are reported in Fig. 20 for two composites with different microstructure, i.e. characterised by the presence of either a platelet or equiaxed Ti_3B_4 phase. At high temperatures, the toughness increases are probably due to plasticity of the TiC_x constituent above its brittle-to-ductile transition temperature. The flexural strength of the composites fabricated by TTPP is insensitive to temperature up to 1000 °C, whereas a significant reduction in strength and a deviation from linearity were observed at 1200 °C. Furthermore, the authors reported evidence of plastic deformation of the $TiC_{0.65}$ constituent by observation of permanent deformation of the samples. A significant strengthening effect was observed in the high-temperature mechanical tests as depicted in Fig. 21, and was attributed to the presence of the boride phases. A direct contribution to the strength from the borides comes from the fact that at high temperature they act as non-yielding particulate reinforcement in a plastic matrix. The authors also suggested some solid-solution strengthening of the TiC_x due to the solubility of boron in titanium carbide. The flexural strength of the composite material at 1000 °C was assumed to increase with the content of the TiB_2 phase. The TiB_2 was in fact the weak link at room temperature because

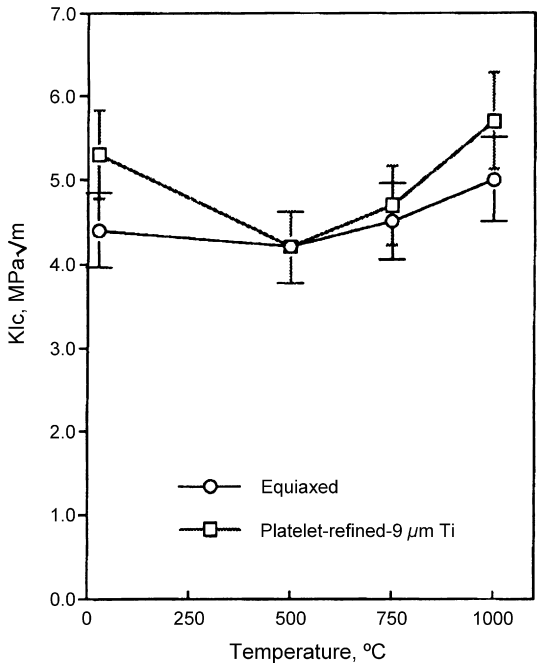

Fig. 20. Variation of the fracture toughness with temperature for platelet and equiaxed TiC–TiB_2–Ti_3B_4 composite fabricated by TPPP.[70]

of the high residual stress induced by its thermal expansion anisotropy. On the other hand, as the strength-governing phase at high temperature was the softer TiC_x, which was the weak link in the microstructure as it deforms plastically, the higher volume fraction of boride resulted in a stronger composite. The platelet composites obtained by TPPP also exhibited thermal shock resistance comparable to similar material, with ΔT_c of 350 °C, which was superior to Al_2O_3–30 vol%TiC cutting tool material (ΔT_c = 150–200 °C[71]). The authors also measured the oxidation resistance of the refined platelet composite. The oxidation was negligible at 750 °C and as a result of the formation of a dense TiO_2–B_2O_3 layer at higher temperatures, the oxidation resistance of the $TiC_{0.65}$–TiB_2–Ti_3B_4 resulted only slightly lower than that of the monolithic fully dense TiB_2.[27] Unfortunately no TiO_2–B_2O_3 binary phase diagram is available to check the stability of composite oxides of the system. However, bearing in mind the relatively low melting point of B_2O_3 (~450 °C), the stability of the TiO_2–B_2O_3 layer cannot be taken for granted.

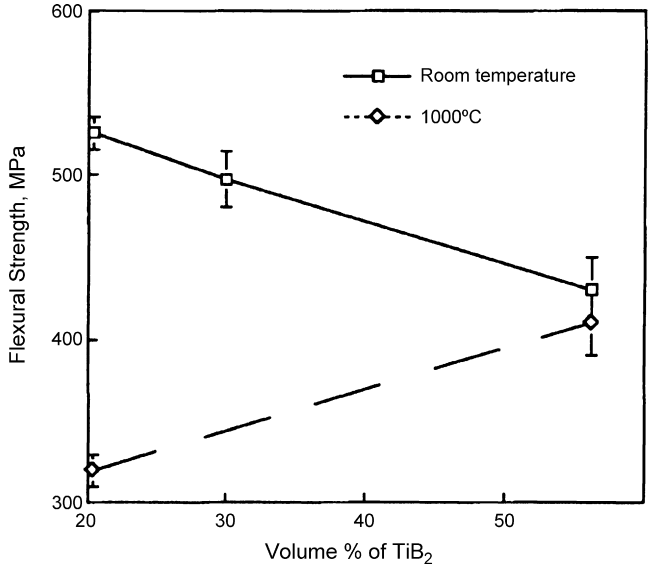

Fig. 21. Variation of the room- and high-temperature flexural strengths of the $TiC_{0.5}$–TiB_2 composite fabricated by TPPP with different carbide:boride mole ratios, with the volume of TiB_2.[70]

A summary of the mechanical properties of TiC–TiB_2 obtained by various processing routes and reported in the literature is summarized in Table 4.

The mechanical properties reported all refer to micron-grained composites, except for those reported by Lee et al.[67] that are measured on nanostructured TiC–TiB_2 composites obtained by field-activation synthesis under pressure from high-energy ball milled elemental reactants. In particular, the authors reported a strong dependence of the composite properties on the milling time, as shown in Fig. 22 for density and hardness.

Since the difference in density between the samples is not significant, the marked change in hardness is attributed to differences in the crystallite size. In accordance with the Hall–Petch relationship[72] the hardness of nanomaterials decreases with an increase in the crystallite size. This is confirmed by the decrease in crystallite size induced by the high-energy milling, that affects the final properties as depicted in Fig. 23 for micro-hardness.

3.2. Application fields for TiC–TiB_2 composites

According to the properties reported in the literature, the potential applications of TiC–TiB_2 composites are high-temperature structural components in heat exchangers and engines, propulsion and space thermal protection in aircraft, wear-resistant parts in cutting tools and forming dies, non-structural applications like wall tiles in nuclear fusion reactors, cathodes in Hall–Heroult cells and vapourising elements in vacuum-metal deposition installations, and coatings for wear- and corrosion-resistant components. Among these, one of the most promising potential applications is for the fabrication of cutting tool inserts. Brodkin et al.[70] have carried out a comparison between TiC–TiB_2 composites and commercial materials

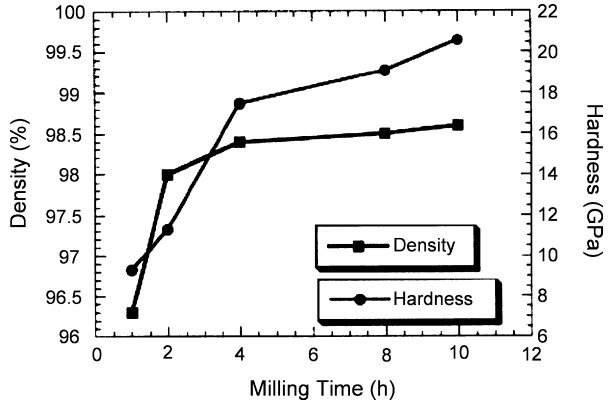

Fig. 22. The dependence of relative density and Vickers micro-hardness of the TiB_2–TiC nanocomposites on prior milling time.[67]

Table 4
Mechanical properties of state-of-the-art TiC/TiB_2–based composites

Material composition	Density or relative density	Vickers hardness (or micro-hardness) (GPa)	Fracture toughness K_{Ic} (MPa $m^{1/2}$)	Bend strength (MPa)	Processing conditions	Ref.
$TiC_x/Ti_3B_4/TiB_2$ (38%:20%:42%)	4.62 g/cm^3	23 ± 3 (10 kg load)	~4	430 ± 30	TPPP 800 °C, 4 h, then 1600 °C, 40 MPa, 4 h	3
$TiC_x/Ti_3B_4/TiB_2$ (35%:33%:32%)	4.59 g/cm^3	19 ± 3 (10 kg load)	~6	630 ± 30	TPPP 800 °C, 4 h, then 1600 °C, 40 MPa, 4 h	3
$TiC_{0.65}/Ti_3B_4/TiB_2$	>99%TD	20 ± 2 (10 kg load)	5.3 ± 0.5	800 ± 30	TPPP 800 °C, 4 h, then 1600 °C, 40 MPa, 4 h	70
$TiC_{0.6}/Ti_3B_4/TiB_2$ (50%:17%: 32%)	>99%TD	18–30 (300 g load)	5.6 ± 0.6	590 ± 30	TPPP 800 °C, 4 h, then 1600 °C, 40 MPa, 4 h	36
TiC/TiB_2 (1:2)	>99%TD	16.2 (20 kg load); 25.4 (micro-hardness, 500 g load)	6.6	210	SHS/TE under pressure, 1000 °C, 150 MPa	4,34,48
TiC/TiB_2 (1:2)	95%TD	15.1 (20 kg load); 20.6 (micro-hardness, 500 g load)	5.9	190	Reactive hot pressing: 1000 °C, 150 MPa, 4 h	4,34,48
TiB_2 + 15%TiC	98.2%TD	22.6	3.5	–	High-pressure sintering (HPS) of premixed TiC/TiB_2 powders, 2250 °C, 3 GPa, 300 s	40
TiB_2 + 15%TiC	99.3%TD	23.9	3.9	–	High-pressure sintering (HPS) of premixed TiC/TiB_2 powders, 2500 °C, 3 GPa, 300 s	40
TiB_2 + 15%TiC	99.1%TD	23.8	4.2	–	High-pressure self-combustion synthesis (HPCS) from T + B + C, 2250 °C, 3 GPa, 300 s	40
TiB_2 + 15%TiC	99.0%TD	23.5	4.6	–	High-pressure self-combustion synthesis (HPCS) from T + B + C, 2500 °C, 3 GPa, 300 s	40
TiC/TiB_2 (1:1)	96.3%TD	9.3 (micro-hardness, 400 g load)	–	–	Field-activated synthesis under pressure (1400 °C, 30 MPa, 3 min) from high-energy ball milled Ti + B + C reactants, 1 h milling	67
TiC/TiB_2 (1:1)	98.6%TD	20.6 (micro-hardness, 400 g load)	–	–	Field-activated synthesis under pressure (1400 °C, 30 MPa, 3 min) from high-energy ball milled Ti + B + C reactants, 10 h milling	67
TiC/TiB_2 (1:2)	–	–	12.2	680	Reactive hot pressing: 1800 °C, 35 MPa, 60 min	[74]74
20TiB_2–80TiC (mol%)	–	25 (10 kg load); 27 (100 g load)	3	–	Floating zone (FZ) directional solidification of TiC/TiB_2 powders isostatically pressed at 40 MPa, and sintered at 1873 K for 3600 s	50
28TiB_2–72TiC (mol%)	–	23 (10 kg load); 26 (100 g load)	4	–		
60TiB_2–40TiC (mol%)	–	20 (10 kg load); 25 (100 g load)	4	–		
TiC/TiB_2 (1:1)	75% TD	–	–	418–940	Pressureless sintering of mixed TiC + TiB_2 powders: 1550 °C, 90 min, Ar	25
TiC/TiB_2 (1:1) + 2.5 wt% (Ni + X)	>90% TD	18.6	7.2	880–1378	Pressureless sintering of mixed TiC + TiB_2 powders: 1550 °C, 90 min, Ar	25
TiC/TiB_2 (1:2) + 15 wt% Ni (1.5 mol)	99%TD	13.8 (20 kg load); 24 (micro-hardness, 500 g load)	11.9	320	SHS/TE under pressure, 1000 °C, 150 MPa	4,34,48
TiC/TiB_2 (1:2) + 15 wt% Ni (1.5 mol)	99%TD	17.6 (20 kg load); 25.7 (micro-hardness, 500 g load)	6.8	260	Reactive hot pressing: 1000 °C, 150 MPa, 4 h	4,34,48

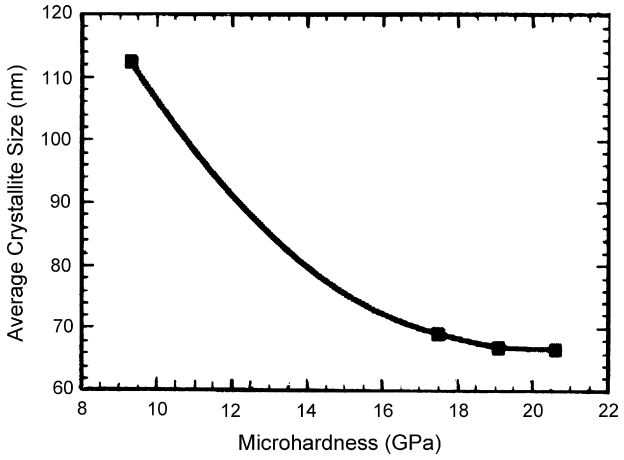

Fig. 23. The relationship between micro-hardness and average crystallite size in dense TiB_2–TiC nanocomposites.[67]

based on the abrasive wear factor (AWF) provided by Evans and Marshall[73] for the evaluation of the wear resistance of ceramic materials. The wear factor can be computed from the fracture toughness (K_{Ic}), Young's modulus (E) and hardness (H). The higher the AWF, the higher the expected resistance of a ceramic material to abrasive wear. The results of the comparison showed that the wear factor of TiC–TiB_2 composites produced by TPPP (AWF = 1.26) favourably compares to commercial Al_2O_3–TiC (1.22) and SiAlON (1.21) cutting tool materials. The good wear resistance of the material was also confirmed from data obtained from abrasive erosion tests by the same authors.[70] It was observed that the wear rate of the TPPP TiC–TiB_2 based composites was comparable to that of SiAlON and WC-Co cutting tool materials.

The available data provide evidence that the combination of good wear resistance and relatively high thermal shock and oxidation resistance renders TiC–TiB_2 composites an excellent candidate for cutting tools. However, no actual application of these materials is commercially available due to the fact that a cost-effective and reliable processing route allowing an accurate control of the microstructure has still to be established for this class of materials. Regarding this, the SHS process seems to offer a promising way provided an accurate control of the process parameters is achieved.

4. Conclusions

TiC–TiB_2 composites are thought to benefit from coherency between the $(1\,1\,1)_{TiC}(0\,0\,0\,1)_{TiB_2}$ interfaces contributing to phase boundary toughening and improved wear resistance in comparison to the monolithic ceramics. Owing to the high melting points of the two constituents, the fabrication of TiC–TiB_2 composites is difficult. The use of a nickel binder together with additives like molybdenum or manganese have been shown to be very effective in obtaining near-net-shape products by means of pressureless sintering. The use of these additives, has been reported to increase the wetting between the ceramic phases and the binder.

SHS and its derivatives where pressure has been applied are capable of yielding products in excess of 95% theoretical density. A lot of the reported studies using SHS have been carried out aiming for a product of eutectic composition in order to promote liquid-phase formation that will assist the sintering process. The variation in the composition of the material can yield significant differences in microstructure. In addition to the eutectic microstructure, spherical TiC grains coexisting with a eutectic mixture are possible at higher TiC content. Products with a higher TiB_2 level have been reported to form prismatic TiB_2 grains together with the eutectic phase. The particle size of the reactant materials plays an important role in the SHS process. Reduction of the reactant particle size leads to an increase in the combustion rate. Reduction of the cooling rate following SHS has been observed to lead to grain growth. An interesting development is the use of the SHS-quench process which results in the formation of a metastable product. Upon heat treatment, morphological evolution of nanocrystalline phases has been observed. Evaluation of the properties of samples produced by these processes, have shown very promising improvements, principally with regard to wear resistance and fracture toughness.

Acknowledgements

This work was carried out in the framework of the FP6 STREP project NAMAMET "Processing of Nanostructured Materials through Metastable Transformations" supported by the European Commission under the contract NMP3-CT-2004-001470. The authors gratefully acknowledge Professor I. Amato for the overview of the technical work.

References

1. Zhao, H. and Cheng, Y., Formation of TiB_2–TiC composites by reactive sintering. *Ceram. Int.*, 1999, **25**, 353–358.
2. Zhou, X., Zhang, S., Zhu, M. and Chen, B., Investigation of TiB_2–TiC composites produced by SHS and their application in Hall–Heroult cells for aluminum electrolysis. *Int. J. Self-Prop. High-Temp. Synth.*, 1998, **7**, 403–408.
3. Brodkin, D., Kalidindi, S., Barsoum, M. and Zavaliangos, A., Microstructural evolution during transient plastic phase processing of titanium carbide–titanium boride composites. *J. Am. Ceram. Soc.*, 1996, **79**(7), 1945–1952.
4. Gutmanas, E. Y. and Gotman, I., Dense high-temperature ceramics by thermal explosion under pressure. *J. Eur. Ceram. Soc.*, 1999, **19**, 2381–2393.
5. Sigl, L. S., Schwetz, K. A. and Dworak, U., Continuous turning with TiB_2 cermets: preliminary cutting tests. *Int. J. Refract. Met. H.*, 1994, **12**, 95–99.
6. Telle, R., Sigl, L. and Takagi, K., Boride-based hard materials. In *Handbook of Ceramic Hard Materials*, ed. R. Riedel. Wiley-VCH, New York, 2003. pp. 880, 927–932.
7. Udwadia, K. K. and Puszynski, J. A., In *In Situ Reactions for Synthesis of Composites, Ceramics and Intermetallics*, ed. E. V. Barrera *et al.* TMS, Warrendale, PA, 1995. p. 59.
8. Frisk, K., A revised thermodynamic description of the Ti–C system. *CALPHAD*, 2003, **27**, 367–373.
9. Dumitrescu, L., Hillert, M. and Sundman, B., Reassessment of Ti–CN based on a critical review of available assessments of Ti–N and Ti–C. *Z. Metallkd.*, 1999, **90**, 534–541.
10. Jonsson, S., Assessment of the Ti–C system. *Z. Metallkd.*, 1996, **87**, 703–772.

11. Jeitschko, W., Pottgen, R. and Hoffman, R. D., Structural chemistry of hard materials. In *Handbook of Ceramic Hard Materials*, ed. R. Riedel. Wiley-VCH, New York, 2003. pp. 9, 12–16.
12. Lipatnikov, V. N., Rempel, A. A. and Gusev, A. I., Atomic ordering and hardness of nonstoichiometric titanium carbide. *Int. J. Refract. Met. H.*, 1997, **15**, 61–64.
13. Tashmetov, M. Y., Em, V. T., Lee, C. H., Shim, H. S., Choi, Y. N. and Lee, J. S., Neutron diffraction study of the ordered structures of nonstoichiometric titanium carbide. *Phys. B*, 2002, **311**, 318–325.
14. Wanjara, P., Drew, R. A. L., Root, J. and Yue, S., Evidence for stable stoichiometric Ti_2C at the interface in TiC particulate reinforced Ti alloy composites. *Acta Mater.*, 2000, **48**, 1443–1450.
15. Ranganath, S. and Subrahmanyam, J., On the in situ formation of TiC and Ti_2C reinforcements in combustion-assisted synthesis of titanium matrix composites. *Metall. Mater. Trans. A*, 1996, **27**, 237–240.
16. Chrysanthou, A., Chen, Y. K., Vijayan, A. and O'Sullivan, J. M., Combustion synthesis and subsequent sintering of titanium-matrix composites. *J. Mater. Sci.*, 2003, **38**, 2073–2077.
17. Lengauer, W., Transition metal carbides, nitrides and carbonitrides. In *Handbook of Ceramic Hard Materials*, ed. R. Riedel. Wiley-VCH, New York, 2003. pp. 202–203, 234–235, 238.
18. Kamal Akhtar, M. and Pratsinis, S. E., Gas phase synthesis processes—thermal aerosol processes. In *Carbide, Nitride and Boride Materials Synthesis and Processing*, ed. A. Weimer. Chapman & Hall, Cambridge, 1997, pp. 333–334.
19. Murray, J. L., Liao, P. K. and Spear, K. E., The Ti–B (titanium–boron) system. *Bull. Alloy Phase Diagrams*, 1986, **7**, 550–555.
20. Murray, J. L., Liao, P. K. and Spear, K. E., The Ti–B (titanium–boron) system. In *Phase Diagrams of Binary Titanium Alloys*, ed. J. L. Murray. ASM International, Metals Park, OH, 1987, pp. 33–38.
21. Spear, K. E., McDowell, P. and McMahon, F., Experimental evidence for the existence of the Ti_3B_4 phase. *J. Am. Ceram. Soc.*, 1986, **69**(1), C-4–C-5.
22. Fenish, R. G., Phase relationships in the titanium–boron system. *NRM*, 1964, **138**, 1–37.
23. Rudy, E. and Windisch, S., *Tech Rep. No. AFML-TR-65-2*, *part II*, *Vol. XIII*, 1966.
24. Thebault, J., Pailler, R., Bontemps-Moley, G., Bourdeau, M. and Naslain, R., Chemical compatibility in boron fiber–titanium composite materials. *J. Less Common Met.*, 1976, **47**, 221–233.
25. Ogwu, A. A. and Davies, T. J., The densification and mechanical properties of a TiC and TiB_2 hardmetal sintered with a reactive alloy binder. *Phys. Status Solidi A-Appl. Res.*, 1996, **153**, 101–116.
26. Holleck, H., Leiste, H. and Shneider, W., In *High Tech Ceramics*, ed. P. Vincenzini. Elsevier Publ. Co., Amsterdam, 1987, pp. 2609–2622.
27. Munro, R. G., Material properties of titanium diboride. *J. Res. Natl. Inst. Stand. Technol.*, 2000, **105**, 709–720.
28. Duschanek, H., Rogl, P. and Lukas, H., A critical assessment and thermodynamic calculation of the boron–carbon–titanium (B–C–Ti) ternary system. *J. Phase Equilib.*, 1995, **16**(1), 46–60.
29. Gusev, A. I., Phase equilibria in the ternary system titanium–boron–carbon: the sections TiC_y–TiB_2 and B_4C_y–TiB_2. *J. Solid State Chem.*, 1997, **133**, 205–210.
30. Brewer, L. and Haraldsen, H., The thermodynamic stability of refractory borides. *J. Electrochem. Soc.*, 1955, **102**, 399–406.
31. Rudy, E., Windisch, S. and Chang, Y.A., *Tech. Rep. No. AFML-TR-65-2*, *part I*, *Vol. I*, 1965.
32. Sorrell, C. C., Beraton, H. R., Bradt, R. C. and Stubican, V. S., Directional solidification of (Ti,Zr) carbide–(Ti,Zr) diboride eutectics. *J. Am. Ceram. Soc.*, 1984, **67**, 190–194.
33. Davies, T. J. and Ogwu, A. A., Characterisation of composite of TiC + TiB_2 bonded with nickel based binder alloy: mechanical and microstructural properties. *Powder Metall.*, 1995, **38**(1), 39–44.
34. Gotman, I., Travitzky, N. A. and Gutmanas, E. Y., Dense in situ TiB_2–TiN and TiB_2–TiC ceramic matrix composites: reactive synthesis and properties. *Mater. Sci. Eng. A-Struct. Mater. Propr. Microstr.*, 1998, **244**, 127–137.
35. Li, J., Li, F., Hu, K. and Zhou, Y., TiB_2/TiC nanocomposite powder fabricated via high energy ball milling. *J. Eur. Ceram. Soc.*, 2001, **21**, 2829–2833.
36. Barsoum, M. W. and Houng, B., Transient plastic phase processing of titanium–boron–carbon composites. *J. Am. Ceram. Soc.*, 1993, **76**(6), 1445–1451.
37. Mogilevsky, P., Werner, A. and Dudek, H. J., Application of diffusion barriers in composite materials. *Mater. Sci. Eng. A-Struct. Mater. Propr. Microstr.*, 1998, **242**, 235–247.
38. Kubaschewski, O. and Alcock, C. B., Thermochemical data. *Metallurgical Thermochemistry*. Pergamon, Oxford, 1979, pp. 258–449.
39. Li, J., Li, F., Hu, K. and Zhou, Y., Formation of TiB_2/TiN/Ti(C_xN_{1-x}) nanocomposite powder via high-energy ball milling and subsequent heat treatment. *J. Alloy Compd.*, 2002, **334**, 253–260.
40. Bhaumik, S. K., Divakar, C., Singh, A. K. and Upadhyaya, G. S., Synthesis and sintering of TiB_2 and TiB_2–TiC composite under high pressure. *Mater. Sci. Eng. A-Struct. Mater. Propr. Microstr.*, 2000, **279**, 275–281.
41. Watanabe, T., Effects of carbide addition on the mechanical properties of Ti($C_{0.5}$, $N_{0.5}$)–30 wt%TiB_2 sintered compacts. *J. Ceram. Soc. Jpn.*, 1991, **99**(2), 142–145.
42. Ogwu, A. A. and Davies, T. J., Developing matrices for hardmetals. In *Proceedings of International Conference on Advances in Hard Materials Production*, Bonn, Germany, 4–6 May 1992. Ed. EPMA, 1992, paper 19.
43. Singh, M., Rai, K. N. and Upadhyaya, G. S., Sintered porous cermets based on TiB_2 and TiB_2–TiC–Mo_2C. *Mater. Chem. Phys.*, 2001, **67**, 226–233.
44. Sacks, M., Bozkurt, N. and Schieffele, G., Fabrication of mullite and mullite-matrix composites by transient viscous sintering of composite powders. *J. Am. Ceram. Soc.*, 1991, **74**(10), 2428–2437.
45. Henager Jr., C. H., Brimhall, J. L. and Hirth, J. P., Synthesis of a $MoSi_2$–SiC composite in-situ using a solid state displacement reaction. *Mater. Sci. Eng. A-Struct. Mater. Propr. Microstr.*, 1992, **155**, 109–114.
46. Hyun, Y. C., Miyamoto, Y., Takano, Y., Koizumi, M. and Yamada, O., Fabrication of TiB_2–TiC ceramic composites by high pressure combustion sintering. In *Proceedings of the First MRS International Meeting on Advanced Materials*, Sunshine City, Ikebukuro, Tokyo, Japan (1988), vol. 5, Structural Ceramics Fracture Mechanics. Material Research Society, Pittsburgh, 1989, pp.119–124.
47. Lee, S. K., Kim, D. and Kim, C. K., Fabrication of TiC/TiB_2 composites by the directional reaction of titanium with boron carbide. *J. Mater. Sci.*, 1994, **29**, 4125–4130.
48. Gutmanas, E. Y. and Gotman, I., Reactive synthesis of ceramic matrix composites under pressure. *Ceram. Int.*, 2000, **26**, 699–707.
49. Hong, F. and Lewis, M. H., Ceramic matrix composites via in-situ reaction sintering. *Ceram. Eng. Sci. Proc.*, 1993, **14**, 699–706.
50. Li, W.-J., Tu, R. and Goto, T., Preparation of directionally solidified TiB_2–TiC eutectic composites by a floating zone method. *Mater. Lett.*, 2006, **60**, 839–843.
51. Miracle, D. and Lipsitt, H., Mechanical properties of fine-grained substoichiometric TiC. *J. Am. Ceram. Soc.*, 1983, **66**(8), 592–596.
52. Munir, Z. A. and Anselmi-Tamburini, U., Self propagating high temperature synthesis of hard materials. In *Handbook of Ceramic Hard Materials*, ed. R. Riedel. Wiley-VCH, New York, 2003, pp. 322–338.
53. Moore, J. J. and Feng, H. J., Combustion synthesis of advanced materials. Part I: Reaction parameters. *Progr. Mater. Sci.*, 1995, **39**, 243–273.
54. Ouabdesselam, M. and Munir, Z. A., The sintering of combustion-synthesized titanium diboride. *J. Mater. Sci.*, 1987, **22**, 1799–1807.
55. Agrafiotis, C. C., Hlavacek, V. and Puszynski, J. A., Direct synthesis of composites and solid solutions by combustion reactions. *Combust. Sci. Technol.*, 1992, **88**, 187–199.
56. Contreras, L., Turrillas, X., Vaughan, G. B. M., Kvick, A. and Rodriguez, M. A., Time-resolved XRD study of TiC–TiB_2 composites obtained by SHS. *Acta Mater.*, 2004, **52**, 4783–4790.
57. Atías Adrián, I. C., Vallauri, D., Zhang, Z., Chrysanthou, A., DeBenedetti, B. and Amato, I., Nanostructured TiC_{1-x}–TiB_2 composites obtained by metastability processing. *Adv. Mater. Res.*, 2006, **15–17**, 225–230.
58. Kear, B. H., Kalman, Z., Sandagi, R. K., Skandan, G., Colaizzi, J. and Mayo, W. E., Plasma-sprayed nanostructured Al_2O_3/TiO_2 powders and coatings. *J. Therm. Spray Technol.*, 2000, **9**, 483–487.
59. Vallauri, D., Atías Adrián, I. C., Deorsola, F. A., Amato, I. and DeBenedetti, B., Metastability route to obtain nanocomposites by SHS. *Int. J. Self-Propagating High-Temp. Synth.*, 2006, **15**(2), 169–179.

60. Tomoshige, R., Kakoki, Y., Imamura, K. and Chiba, A., Effect of addition of titanium diboride to titanium carbide produced by the SHS—shock consolidation method. *J. Mater. Process. Technol.*, 1999, **85**, 105–108.
61. Fu, Z. Y., Wang, H., Wang, W. M. and Yuan, R. Z., Composites fabricated by self-propagating high-temperature synthesis. *J. Mater. Process. Technol.*, 2003, **137**, 30–34.
62. Xinghong, Z., Chungcheng, Z., Wei, Q. and Kvanin, V. L., Self-propagating high temperature combustion synthesis of TiC/TiB_2 ceramic-matrix composites. *Compos. Sci. Technol.*, 2002, **62**, 2037–2041.
63. Wang, L., Wixom, M. R. and Thompson, L. T., Structural and mechanical properties of TiB_2 and TiC prepared by self-propagating high-temperature synthesis/dynamic compaction. *J. Mater. Sci.*, 1994, **29**, 534–543.
64. Kecskes, L. J., Kottke, T. and Niiler, A., Microstructural properties of combustion-synthesised and dynamically consolidated titanium boride and titanium carbide. *J. Am. Ceram. Soc.*, 1990, **73**(5), 1274–1282.
65. Klinger, L., Gotman, I. and Horvitz, D., In situ processing of TiB_2/TiC ceramic composites by thermal explosion under pressure: experimental study and modelling. *Mater. Sci. Eng. A-Struct. Mater. Propr. Microstr.*, 2001, **302**, 92–99.
66. Laskar, A. L., Bocquet, J. L., Brebec, G. and Monty, C., *Diffusion in Materials*. Kluwer, Dordrecht, The Netherlands, 1990.
67. Lee, J. W., Munir, Z. A. and Ohyanagi, M., Dense nanocrystalline TiB_2–TiC composites formed by field activation from high-energy ball milled reactants. *Mater. Sci. Eng. A-Struct. Mater. Propr. Microstr.*, 2002, **325**, 221–227.
68. Holleck, H., Leiste, H. and Schneider, W., Significance of phase boundaries in wear resistant TiC/TiB_2 materials. Part 1: Investigations with transmission electron microscopy. *Int. J. Refract. Met. H.*, 1987, **6**(3), 149–154.
69. Davies, T. J. and Ogwu, A. A., TiC + TiB_2 composite shows wear promise. *Met. Powder Rep.*, 1997, **52**, 31–34.
70. Brodkin, D., Zavaliangos, A., Kalidindi, S. and Barsoum, M., Ambient- and high-temperature properties of titanium carbide–titanium boride composites fabricated by transient plastic phase processing. *J. Am. Ceram. Soc.*, 1999, **82**(3), 665–672.
71. Wayne, S. F. and Buljian, T., The role of thermal shock on tool life of selected ceramic cutting tool materials. *J. Am. Ceram. Soc.*, 1989, **72**(5), 754–760.
72. Hertzberg, R. W. and Deformation, *Fracture Mechanics of Engineering Materials* (*3rd ed.*). Wiley, New York, 1989.
73. Evans, A. G. and Marshall, D. B., Wear mechanisms in ceramics. In *ASM Fundamentals of Friction and Wear of Materials*, ed. D. A. Rigney. ASM International, Metals Park, OH, 1981, pp. 439–452.
74. Wen, G., Li, S. B., Zhang, B. S. and Guo, Z. X., Reaction synthesis of TiB_2–TiC composites with enhanced toughness. *Acta Mater.*, 2001, **49**, 1463–1470.